LYMPHOID NEOPLASIA

UCH-L1 is induced in germinal center B cells and identifies patients with aggressive germinal center diffuse large B-cell lymphoma

Tibor Bedekovics,[1] Sajjad Hussain,[1] Andrew L. Feldman,[2] and Paul J. Galardy[1,3,4]

[1]Department of Pediatric and Adolescent Medicine, [2]Department of Pathology and Laboratory Medicine, [3]Division of Pediatric Hematology-Oncology, and [4]Department of Biochemistry and Molecular Biology, Mayo Clinic, Rochester, MN

Key Points

- The neuronal marker UCH-L1 is induced in, and specifically augments the oncogene-induced transformation of, GCB cells.
- High levels of *UCHL1* identify patients with GC DLBCL with an increased risk for poor outcomes.

Gene expression profiling has identified 2 major subclasses of diffuse large B-cell lymphoma (DLBCL). Cases resembling germinal center (GC) B cells (GCB-DLBCL) generally occur in younger patients, have a distinct molecular pathophysiology, and have improved outcomes compared with those similar to activated post-GC cells (activated B-cell DLBCL). We previously found that the ubiquitin hydrolase UCH-L1 is frequently overexpressed in mature B-cell malignancies and is a potent oncogene in mice. The cause for its overexpression in lymphoma, and whether it impacts the outcome of patients with DLBCL is unknown. Here, we show that UCH-L1 reflects GC lineage in lymphoma and is an oncogenic biomarker of aggressive GCB-DLBCL. We find that UCH-L1 is specifically induced in GC B cells in mice and humans, and that its expression correlates highly with the GCB subtype in DLBCL. We also find that UCH-L1 cooperates with *BCL6* in a mouse model of GC B-cell lymphoma, but not with the development of multiple myeloma derived from post-GC cells. Despite the typically good outcomes of GCB-DLBCL, increased *UCHL1* identifies a subgroup with early relapses independent of *MYC* expression, suggesting biological diversity in this subset of disease. Consistent with this, forced *Uchl1* overexpression had a substantial impact on gene expression in GC B cells including pathways of cell cycle progression, cell death and proliferation, and DNA replication. These data demonstrate a novel role for UCH-L1 outside of the nervous system and suggest its potential use as a biomarker and therapeutic target in DLBCL. (*Blood*. 2016;127(12):1564-1574)

Introduction

Germinal center (GC) and post-GC-derived B-cell malignancies comprise an important group of cancers that affect children and adults. Diffuse large B-cell lymphoma (DLBCL) can be subclassified based on gene expression signatures into GC B-cell (GCB) or activated B-cell (ABC) types that reflect a GC or post-GC cell of origin, respectively.[1] Although associated with superior outcomes,[1] many patients with GCB-DLBCL experience relapse of their disease and the overall survival of recurrent DLBCL of any subtype is poor.[2,3]

Through an unbiased activity screen of deubiquitinating enzymes in a variety of cancers, we uncovered frequent overexpression of the neuroendocrine-specific enzyme UCH-L1 in mature B-cell cancers including Burkitt lymphoma and DLBCL.[4,5] We subsequently found transgenic *Uchl1* drives the development of spontaneous lymphoma in mice, demonstrating its oncogenic activity.[5] Mechanistically, UCH-L1 plays a novel role in regulating mammalian target of rapamycin (mTOR)-AKT signaling, a pathway important in GCB and lymphoma development.[6,7] Despite its frequent overexpression, there are no chromosome translocations, copy number alterations, or point mutations known to affect UCH-L1 levels. Here, we report that UCH-L1 expression is specifically induced in GC B cells, and its expression reflects GC identity in lymphoma. Forced expression of UCH-L1 promotes oncogenic gene expression patterns in GC B cells and accelerates lymphomagenesis driven by the GC regulator and oncogene BCL6. Importantly, we find that increased *UCHL1* identifies patients with a poor prognosis specifically in GCB-DLBCL. We conclude that UCH-L1 expression in lymphoma reflects GCB gene expression patterns in lymphoma and may represent a novel prognostic marker and therapeutic target in this disease.

Methods

Reagents and general procedures

Antibodies include BCL6 (Santa Cruz Biotechnology, Dallas, TX, and Cell Signaling Technology, Danvers, MA), IRF4, Histone H2B, Tubulin, p-AKT^{S473}, AKT (Cell Signaling Technology), BCL2 (R&D Systems, Minneapolis, MN), B220, GL7, IgG1, and CD138 (BD Pharmingen, San Jose, CA), CD23, and UCH-L1 (Thermo Scientific, Waltham, MA). Biotin-conjugated secondary antibodies were from Vector Laboratories (Burlingame, CA). Cells were cultured in complete RPMI 1640 (high glucose with pyruvate and glutamine) supplemented with 10% stem cell qualified fetal bovine serum (Gemini Bio-Products, West Sacramento, CA). Lentivirus-encoded

Submitted July 9, 2015; accepted December 21, 2015. Prepublished online as *Blood* First Edition paper, December 23, 2015; DOI 10.1182/blood-2015-07-656678.

The online version of this article contains a data supplement.

There is an Inside *Blood* Commentary on this article in this issue.

The publication costs of this article were defrayed in part by page charge payment. Therefore, and solely to indicate this fact, this article is hereby marked "advertisement" in accordance with 18 USC section 1734.

Table 1. Characteristics of *UCHL1*-expressing lymphomas

Characteristic	All	*UCHL1* HI (80%-100%) No. (%)	*P*
Total	215	43	
Morphologic Dx			<.0001
DLBCL	162 (75)	15 (35)	
BL	8 (4)	6 (14)	
Atypical BL	28 (13)	17 (40)	
Unclassified aggressive mature B-NHL	18 (8)	5 (11)	
GEP			.0012
ABC	55 (26)	3 (7)	
GCB	117 (54)	35 (81)	
Unclassified	43 (20)	5 (12)	
Mol. Dx.			<.0001
mBL	44 (21)	32 (74)	
Non-mBL	125 (58)	8 (19)	
Intermediate	46 (21)	3 (7)	
BCL2 IHC			<.0001
Absent	61 (29)	26 (60)	
Present	149 (69)	15 (35)	
NA	5 (2)	2 (5)	
BCL6 IHC			.0435
Absent	29 (13)	2 (5)	
Present	165 (77)	40 (93)	
NA	21 (10)	1 (2)	
BCL6 break			.0405
Absent	173 (80)	41 (95)	
Present	36 (17)	2 (5)	
NA	6 (3)	0 (0)	
IgH-BCL2 fusion			NS
Absent	188 (87)	38 (88)	
Present	25 (12)	5 (12)	
NA	2 (1)	0 (0)	
MYC status			<.0001
MYC neg.	139 (65)	10 (24)	
Ig-MYC	57 (26)	31 (72)	
Non-Ig-MYC	15 (7)	1 (2)	
NA	4 (2)	1 (2)	

Data extracted from GEO dataset GSE4475.

B-NHL, B-cell non-Hodgkin's lymphoma; BL, Burkitt lymphoma; Dx, diagnosis; IHC, immunohistochemistry; Mol. Dx., molecular diagnosis; NA, not applicable; neg., negative; NS, not significant.

short-hairpin RNAs (shRNAs) were generated and used as described.[5,8] Cell viability was monitored using the MTS (3-(4,5 dimethylthiazol-2-yl)-5-(3-carboxymethoxyphenyl-2-(4-sulfophenyl)-2H-tetrazolium) assay as described.[5,8] Flow cytometry was performed and analyzed with an Accuri C6 cytometer (Accuri Cytometers Inc, Ann Arbor, MI), using BD Accuri C6 software version 1.0.264.21. Quantitative real-time polymerase chain reaction (PCR) was performed using TaqMan probes for mouse *Uchl1* normalized to *Gapdh* (Applied Biosystems). Fold-change was calculated with the Δ-Δ cycle threshold method. Tumor clonality was determined as described.[9,10]

Mice, immunizations, isolation of GCBs, and antigen-specific immunity

Uchl1^{Tg},[5] IμHABCL6,[10] and Vk*MYC mice[11] were housed in barrier conditions in accordance with protocols approved by the institutional animal care and use committee of the Mayo Clinic. GCB and non-GCB isolation was carried out as described[12] and purity confirmed by flow cytometry (BD Accuri C6; BD Biosciences, San Jose, CA). To monitor antigen-specific immune responses, mice (3-4 months of age) were immunized with 4-Hydroxy-3-nitrophenylacetyl hapten conjugated to keyhole limpet hemocyanin (NP-KLH; Biosearch Technologies, Petaluma, CA) in Freund complete adjuvant (Sigma). Enzyme-linked immunosorbent assay (ELISA) plates coated with NP(25)-bovine serum albumin (Biosearch) were incubated with a 1/5000 dilution of serum samples collected on days 0, 7, and 14. Captured molecules where detected by horseradish peroxidase–conjugated anti-mouse immunoglobulin G1 (IgG1).

Histology and immunohistochemistry

Formalin-fixed paraffin-embedded tissues were used for histology, immunohistochemistry, and immunofluorescence. Antigen retrieval was performed with the Vector Antigen Unmasking Solution (Vector Laboratories, Burlingame, CA). Slides were developed by diaminobenzidine (Vector Laboratories) or fluorescent-labeled secondary antibodies (R&D Systems). The terminal deoxynucleotidyl transferase dUTP nick-end labeling (TUNEL) assay was performed using the TACS In situ Apoptosis Detection kit (Trevigen Inc, Gaithersburg, MD). The tissue microarray was created as part of the Mayo Clinic Lymphoma Specialized Program of Research Excellence (SPORE) Molecular Epidemiology Resource, a prospective cohort of over 5000 lymphoma patients. All research involving human samples was reviewed and approved by the Mayo Clinic Institutional Review Board.

Analysis of gene expression data and statistics

RNA was isolated using RNeasy (Qiagen) from GCB from IμHABCL6 or *Uchl1*^{Tg}/IμHABCL6 mice (n = 3 each); gene expression was measured on an Affymetrix Mouse 430 2.0 array through the Mayo Clinic Gene Expression Core. All samples were preprocessed and normalized using Partek software. Robust multiarray average normalization was applied to the samples and the expression signals were converted to log2 scale for downstream analysis. The data were analyzed for quality control using principal component analysis and hierarchal clustering from Partek. The standard analysis of variance model from Partek was applied to calculate the differentially expressed genes for each of the comparisons. Gene expression and clinical annotations from GSE2350,[13] GSE4475,[14] GSE31312,[15] GSE36133[16] (human), and GSE38696, GSE38697[17] GSE39403,[18] GSE38304[19] (mouse) were extracted from the NCBI Gene

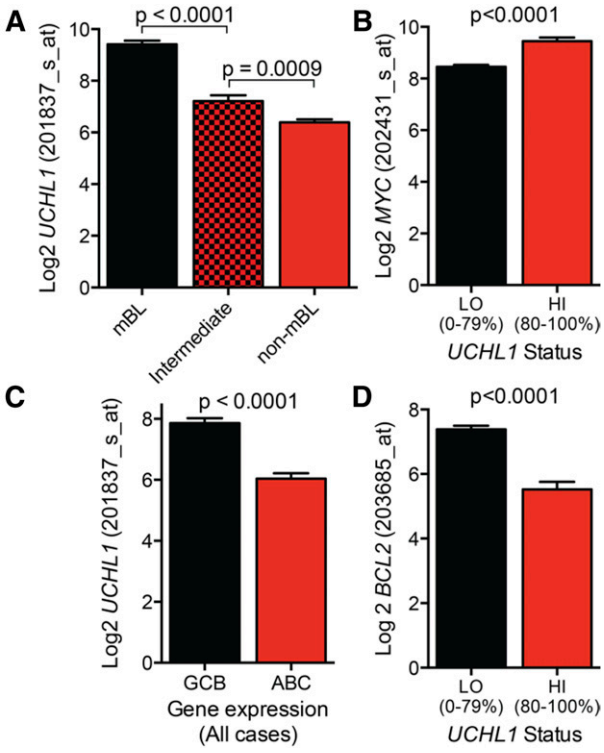

Figure 1. *UCHL1* expression is highest in GCB-derived lymphomas. (A,C) The expression of *UCHL1* as reflected in RNA microarray data are shown for a series of 215 cases of mature B-cell lymphoma classified based on molecular classification as either mBL, non-mBL, or intermediate (A) or cell-of-origin gene expression classification including both mBL and non-mBL cases (C). (B,D) Expression of *MYC* (B) or BCL2 (D) in cases from panel A classified based on the level of *UCHL1* as shown. Data were extracted from GSE4475[14] and analyzed using the R2: Genomics Analysis and Visualization Platform (http://r2.amc.nl). All *P* values were calculated using the Student *t* test.

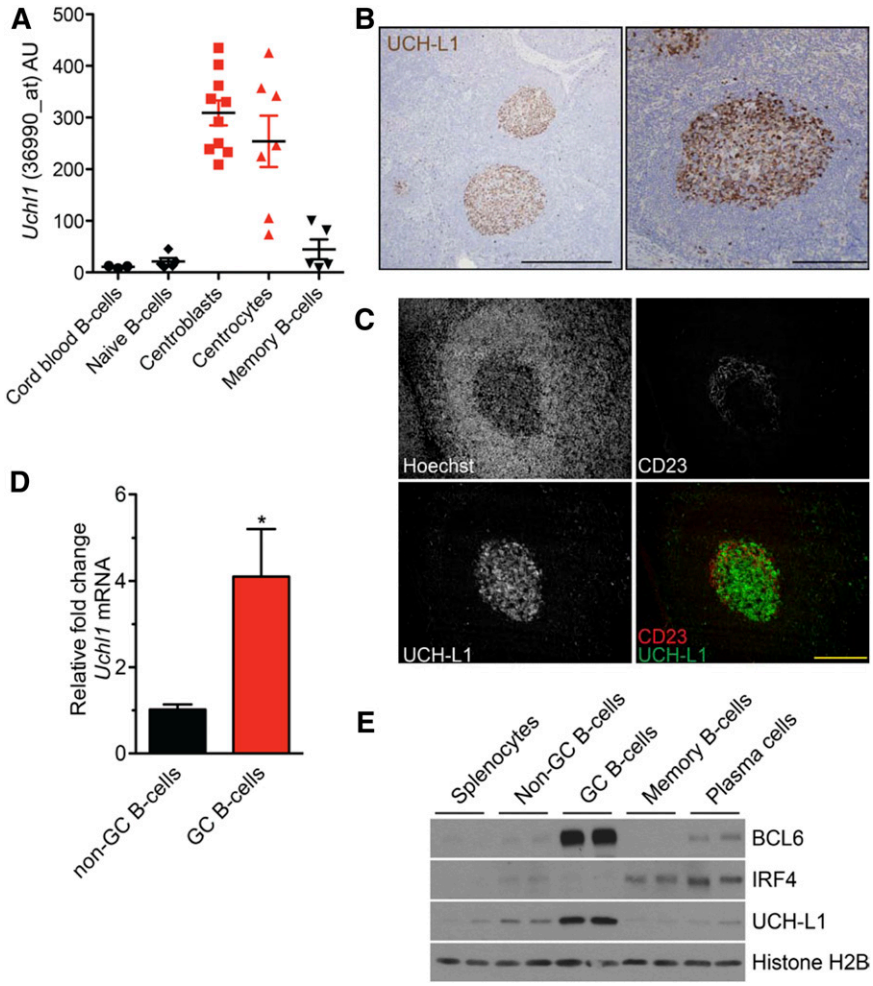

Figure 2. UCH-L1 is specifically induced in GCBs. (A) The expression of *UCHL1* as reflected in RNA microarray data are shown for the indicated purified human B-cell subsets. Data extracted from GSE2350.[13] (B) Formalin-fixed paraffin-embedded human reactive lymph node specimens were stained for UCH-L1 (brown). Bar: 500 μm (left), 200 μm (right). (C) Formalin-fixed paraffin-embedded human tonsil sections were stained with the indicated. Bar: 200 μm. (D) Quantitative real-time PCR for murine *Uchl1* was performed on complementary DNA generated from GC or non-GCBs purified from wild-type mice (n = 3 each); $^*P < .05$. (E) Extracts were prepared from the indicated purified B-cell subsets (n = 2 each), and samples were immunoblotted for the indicated proteins. Histone H2B is included as a loading control. Microscopy images were obtained with an Olympus AX70 microscope with a DP71 camera.

Expression Omnibus (GEO) database and analyzed using the R2: Genomics Analysis and Visualization Platform (http://r2.amc.nl). Normalized log2 transformed gene expression data were downloaded from the R2 platform to a Microsoft Excel spreadsheet for additional analysis. All statistics were performed using GraphPad Prism software with the exception of the univariate and multivariate analyses, which were performed using JMP (SAS).

Results

UCH-L1 overexpression is characteristic of Burkitt lymphoma and GCB-DLBCL

To understand its impact on aggressive B-cell lymphomas, we developed a profile of UCH-L1–expressing lymphomas. We classified 215 cases of B-cell lymphoma as either *UCHL1* LO (0%-79%) or *UCHL1* HI (80%-100%) based on gene expression profiling.[14] Comparing the *UCHL1* HI cases with the overall cohort, there was a highly significant difference in the morphologic classification, with *UCHL1* HI cases more likely to have a Burkitt or atypical Burkitt histology (Table 1). Of those classified as DLBCL, there was a significant enrichment ($P = .007$) of cases with the GCB signature. Within the *UCHL1* HI cases, there was also a significant increase in cases molecularly classified as Burkitt lymphoma (mBL). Consistent with this, *UCHL1* HI cases were significantly more likely to carry the immunoglobulin-*MYC* translocation (Table 1). There was also a significant difference in immunohistochemical patterns, as *UCHL1* HI cases were more likely to be BCL2-negative, BCL6-positive, and less likely to have a break in the *BCL6* locus (Table 1).

To complement these data, we examined the gene expression profiles (GEPs) of these cases. Cases classified as mBL by GEP had a significantly higher level of *UCHL1* compared with either non-mBL or intermediate cases (Figure 1A). As expected based on the enrichment of mBL and immunoglobulin-MYC translocations, *UCHL1* HI tumors had significantly increased *MYC* expression (Figure 1B). Cases classified as GCB also had a significant increase in *UCHL1* compared with ABC (Figure 1C). As predicted by immunohistochemistry, there was a significantly lower mean *BCL2* level by gene expression profiling in those cases with high *UCHL1* (Figure 1D). To further verify the expression of UCH-L1 in DLBCL, we performed immunohistochemistry on a tissue microarray containing 250 cases of DLBCL (149 GCB). Of these cases, a total of 151 (60%) had at least some immunoreactivity for UCH-L1 and 33 (13%) had strong immunoreactivity (supplemental Figure 1A-C, available on the *Blood* Web site). In 104 cases (42% of the total cases; 69% of those with any immunoreactivity), the percentage of immunopositivity was <50% of the tumor cells. There was a significant increase in the number of positive cases in the GCB group (68% vs 53%; $P = .05$). These data demonstrate that UCH-L1 protein is detectable by immunohistochemistry in DLBCL. Taken together, we conclude that B-cell lymphomas that express high levels of UCH-L1 are likely

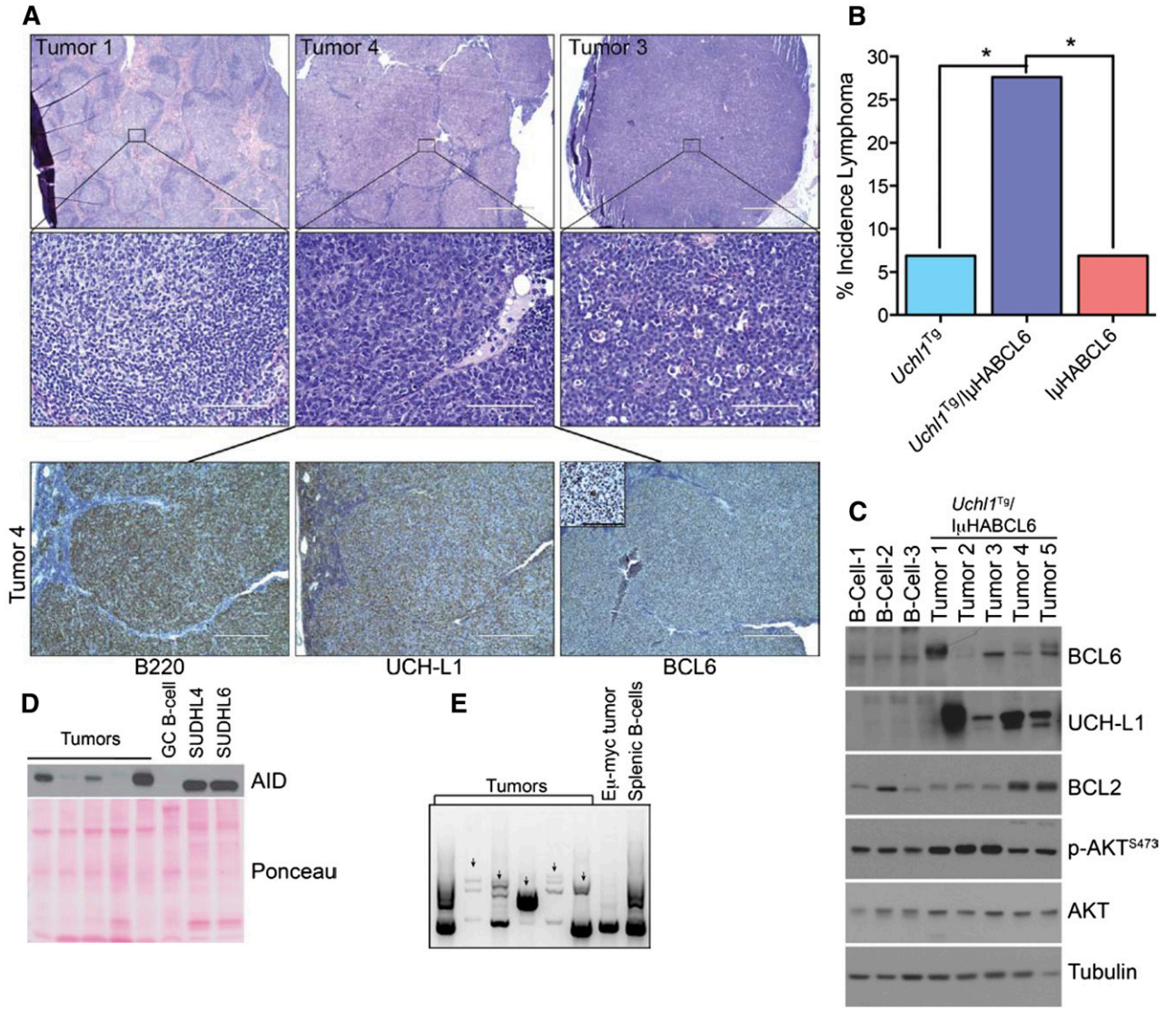

Figure 3. Transgenic UCH-L1 synergizes with deregulated BCL6 in the development of B-cell lymphoma. (A) Representative histology of lymphomas observed in *Uchl1*^{Tg}/IμHABCL6 mice. Formalin-fixed paraffin-embedded sections were stained with hematoxylin and eosin (top 2 rows) or immunohistochemistry (bottom row) with antibodies against the indicated antigens. Bar: 1000 μm (top row), 100 μm (middle row), 400 μm (bottom row), 100 μm (inset, bottom row). Microscopy images were obtained with an Olympus AX70 microscope with a DP71 camera. (B) The incidence of lymphomas is shown for the indicated mouse strains. *$P < .05$ as determined with the χ^2 test; N = 29 mice for each genotype. (C-D) Immunoblots were performed on extracts from lymphomas as in panel A. Comparison is made with purified B cells (C), purified GCBs (D) from the spleens of wild-type littermates, or the indicated GCB-DLBCL cell lines (D). (E) Genomic DNA was extracted from the indicated samples and subjected to PCR amplification of immunoglobulin variable regions. The arrows denote unique monoclonal bands not seen in the polyclonal B cells.

to have gene expression and immunophenotypic characteristics of GC lineage.

UCH-L1 is expressed in GCBs

The mechanisms for increased UCH-L1 expression in lymphoma are not clear. According to the COSMIC database (http://cancer.sanger.ac.uk/cosmic), there are no reported mutations or chromosome alterations that involve the *UCHL1* locus, suggesting direct transcriptional regulation. Although UCH-L1 is widely regarded as a neuroendocrine-specific enzyme,[20] we reasoned that whole-tissue GEP might easily miss its expression in the relatively small population of GCB. We therefore examined data from purified human B-cell populations.[13] Although *UCHL1* levels were very low in naive and memory B cells, its expression sharply increased in centroblast and centrocyte GCB populations (Figure 2A). Strikingly, there is a very similar pattern of expression in cancer cell lines derived from these stages of development (supplemental Figure 2).[5,16] We next performed immunohistochemistry on human reactive lymph nodes and found a striking localization of UCH-L1 protein to GCs (Figure 2B). There was no evidence of polarized expression between the light and dark zones (Figure 2C). Consistent with this, *UCHL1* messenger RNA (mRNA) was not substantially different in these populations in either human or mouse (supplemental Figure 3).[17] We also found high levels of *Uchl1* mRNA and protein in purified GCB from mice (Figure 2D-E), and the strong induction of UCH-L1 expression in B cells undergoing an in vitro class switch recombination assay (supplemental Figure 4A-B). The expression of UCH-L1 in GC B cells is not induced by BCL6, as purified GCB from mice with deregulated expression of BCL6 (IμHABCL6)[10] do not have higher levels of UCH-L1 (supplemental Figure 5A). In previous studies, neither BCL6 depletion, nor the overexpression of degradation-deficient BCL6, changed *UCHL1* levels.[21,22] Published

chromatin immunoprecipitation–sequencing (ChIP-seq) data did not find BCL6 occupancy of the *UCHL1* promoter.[23] We also examined whether UCH-L1 was induced by MYC. Two independent studies using *Myc*–green fluorescent protein (GFP) reporter mouse strains recently examined the role of MYC in GCB development.[18,19] In these reports, gene expression in Myc-GFP-negative or -positive purified GCB showed no changes in *Uchl1* transcript level[18,19] (supplemental Figure 5B), providing compelling evidence that MYC does not induce UCH-L1 expression. Taken together, these data demonstrate that UCH-L1 is specifically induced in GCB, and suggest that its expression in B-cell lymphoma reflects its expression in the cell or origin.

UCH-L1 accelerates BCL6-driven B-cell lymphomagenesis

To further examine its impact on GC-derived lymphomagenesis, we crossed transgenic mice that express UCH-L1 in a broad tissue distribution ($Uchl1^{Tg}$)[5] with mice carrying deregulated *BCL6*.[10] In this model, HA-tagged BCL6 was inserted into the immunoglobulin heavy chain enhancer (IμHABCL6). We generated cohorts of *Uchl1*, IμHABCL6, and *Uchl1*/IμHABCL6 double mutant mice and analyzed them for lymphomas. As expected based on their young age, there was a low rate of B-cell lymphoma in either the *Uchl1* or IμHABCL6 strains (Figure 3A-B). However, we observed a significant increase in lymphomagenesis in the double mutant mice. The tumors were of B-cell lineage, and exhibited a range in histology spanning from follicular-type lymphomas to DLBCLs (Figure 3C). As has been reported previously, BCL6 expression is difficult to detect in some tumors using immunohistochemistry, though BCL6 and UCH-L1 protein was seen in all cases by immunoblotting (Figure 3C). Of the 5 tumors analyzed, 3 had increased levels of p-AKT^{S473} and 2 had increased BCL2. The tumors also expressed substantial amounts of activation-induced cytidine deaminase (Figure 3D). Clonality of the tumors was confirmed by immunoglobulin PCR (Figure 3E). Taken together, these data demonstrate that UCH-L1 cooperates with BCL6 in B-cell lymphomagenesis.

We next tested whether UCH-L1 also accelerates the development of myeloma. To address this, we mated $Uchl1^{Tg}$ mice with a transgenic model in which the human *MYC* oncogene is driven by the mouse κ light-chain locus (Vk*MYC).[11] With age, these animals develop multiple myeloma with biological features that closely resemble human disease. Consistent with prior reports, Vk*MYC mice develop *m*-spikes prior to 20 weeks of age with the incidence reaching 100% by 80 weeks, with nests of $CD138^+$ cells in the bone marrow of affected mice consistent with transformed plasma cells (supplemental Figure 6A-B). The onset and progression of *m*-spike development was unchanged in Vk*MYC/$Uchl1^{Tg}$ double mutant mice. We additionally found no UCH-L1–associated changes in the numbers of marrow plasma cells, serum IgG, or blood hemoglobin (a sign of end organ dysfunction) in these mice (supplemental Figure 6C-E). We conclude that UCH-L1 specifically cooperates with the generation of cancers derived from GCBs.

UCH-L1 is a prognostic marker in GC-derived B-cell lymphomas

To assess whether UCH-L1 expression has an impact on outcomes, we turned to a clinically annotated gene expression data set[14] of 155 cases with paired GEP and outcome data consisting of 30 cases of mBL, 92 non-mBL, and 33 intermediate defined by GEP. Within the mBL group, most samples have high levels of *UCHL1*, as seen in Table 1. There was no difference in outcome in mBL cases with low (n = 7) vs those with high levels (n = 23) (data not shown). We next analyzed the outcomes in those patients with non-mBL, with *UCHL1* HI defined as the top 20% of the expression range within this subgroup (n = 17). There was a highly significant and substantial reduction in survival in the *UCHL1* HI cohort compared with the remaining patients (Figure 4).

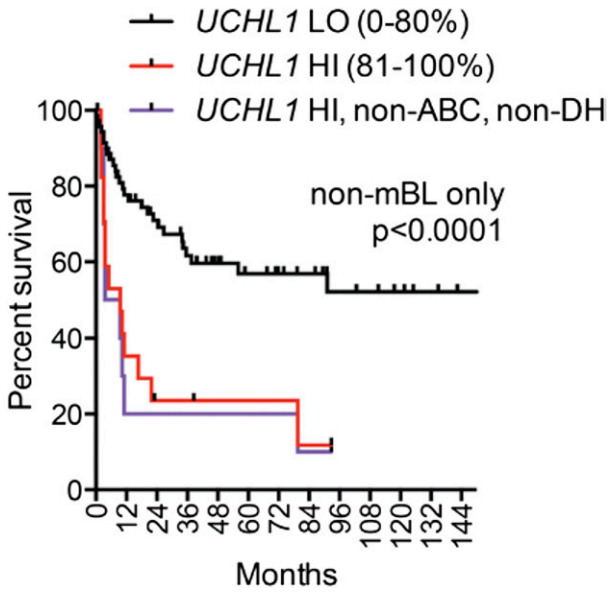

Figure 4. High levels of UCHL1 mark patients with non-mBL at high risk for relapse. Overall survival is plotted using the Kaplan-Meier method for 92 patients with non-mBL stratified based on the level of *UCHL1* mRNA as shown. Those with ABC gene expression profile and double hit (DH) lymphoma (as defined by reported fluorescence in situ hybridization studies for *MYC*, *BCL2*, and *BCL6*) were excluded as shown. Data were extracted from GSE4475[14] and analyzed using the R2: Genomics Analysis and Visualization Platform (http://r2.amc.nl). *P* value was determined using the Mantel-Cox log-rank test.

Two factors known to have a powerful impact on outcomes include ABC GEP and so called "double-hit" lymphoma, defined as the combined occurrence (any 2) of *MYC*, *BCL2*, or *BCL6* rearrangements.[24] Of the patients with increased *UCHL1*, there were 4 ABC subtypes and 3 double hit cases. If these 7 patients are removed, the survival remains severely inferior, indicating that the negative impact of high *UCHL1* expression is independent of these known poor prognostic factors (Figure 4). Although the patient cohort was not uniformly treated, most (75%) received a "CHOP-like" regimen, and 16% received rituximab.

To examine impact of UCH-L1 in patients treated with modern therapy, we turned to the International DLBCL Rituximab-CHOP Consortium Program, a data set containing 470 patients with DLBCL uniformly treated with rituximab with cyclophosphamide, doxorubicin, vincristine, and prednisone (R-CHOP) and having clinical data and GEP.[15] Examining the cohort without regard to cell of origin revealed that increased levels of *UCHL1* (80%-100%) were associated with a significant reduction in progression-free survival (PFS) (Figure 5A). Comparing the *UCHL1* LO and HI groups, there was no difference in clinical stage or the proportion of patients with high International Prognostic Index (IPI) scores (supplemental Figure 7A-B). We again observed a significant increase in *UCHL1* HI cases classified as GCB subtype (supplemental Figure 7C). Subgroup analysis revealed a highly significant negative impact of increased *UCHL1* on PFS in the GCB subgroup, but not in the ABC group (Figure 5B-C). As seen in the other cohort, there was an increase in *MYC* in the *UCHL1* HI cases (Figure 5D). Strikingly, patients with increased *MYC* (75%-100% expression range) and *UCHL1* had a far worse outcome compared with increased *MYC* alone (Figure 5E). Additionally, the negative impact of high *MYC* on outcome was entirely lost in cases with low *UCHL1* (Figure 5F). To further explore the relationship between *UCHL1* and *MYC*, we conducted univariate and multivariate analysis. For the univariate analysis, we also analyzed the impact of *EZH2* levels as high levels were recently found to be favorable in GCB-DLBCL.[25] As

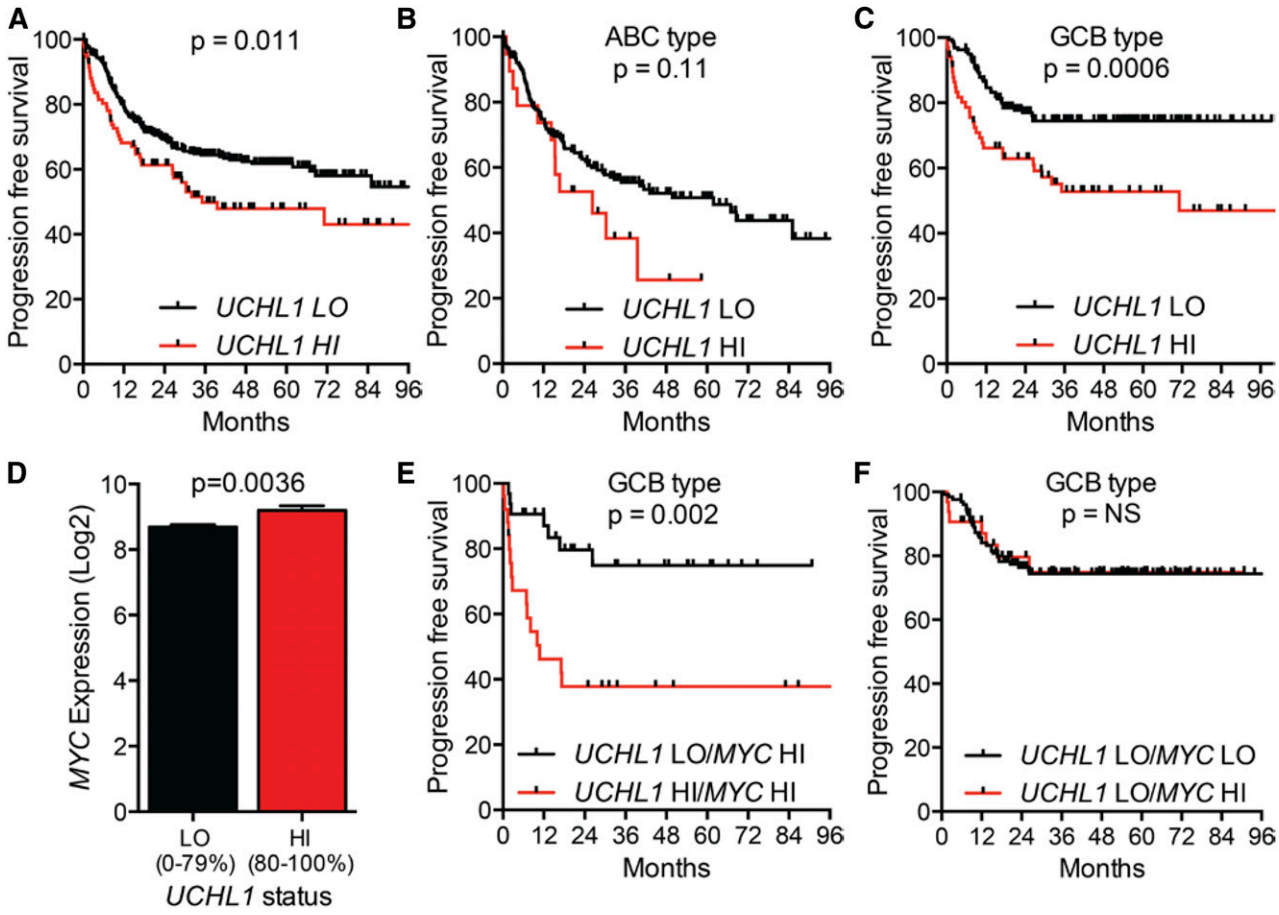

Figure 5. High levels of UCHL1 predict poor outcomes in patients with GCB-DLBCL treated with R-CHOP. (A-C) PFS for all patients with paired gene expression and survival data from the International DLBCL Rituximab-CHOP Consortium Program study (n = 470) (A), those with ABC-DLBCL (n = 199) (B), and GCB-DLBCL (n = 227) (C). *UCHL1* was stratified with LO (=0%-80%) HI (=80%-100%) based on the entire cohort. *P* values were determined using the Mantel-Cox log-rank test. (D) The level of *MYC* mRNA is shown for the entire cohort from panel A including those lacking survival data (n = 498). *UCHL1* stratification as in panels A-C. *P* value was determined using the Student *t* test. (E-F) PFS of patients with GCB-DLBCL (n = 227) with paired gene expression and survival data based on the stratification of *UCHL1* and *MYC*. *UCHL1* was stratified as above. *MYC* was stratified with LO (=0%-75%) and HI (=75%-100%). Data extracted from GSE31312 and analyzed using the R2: Genomics Analysis and Visualization Platform (http://r2.amc.nl).

expected, high levels of *MYC*, *UCHL1*, and low levels of *EZH2* (<85% maximum) all had a significant impact on PFS in the univariate analysis, and all continued to be significant on multivariate analysis (Tables 2-3). We conclude that *UCHL1* and *MYC* have an additive impact on outcome, suggesting independent mechanisms in the pathophysiology of GCB-DLBCL.

UCH-L1 promotes mTORC2 activity, AKT phosphorylation, and cell survival in DLBCL

We previously observed that UCH-L1 affects the stability of mTOR complex 1 (mTORC1) resulting in increased formation of mTORC2 and enhanced phosphorylation of AKT^{S473}.[5,8] To determine whether a similar mechanism operates in DLBCL cells, we examined the expression of *UCHL1* in the cancer cell line encyclopedia (CCLE; http://www.broadinstitute.org/ccle/home) and identified a set of GCB-DLBCL cell lines with varied expression of *UCHL1*, the pattern of which we confirmed by immunoblotting (Figure 6A-B). We used a set of doxycycline (Dox)-inducible shRNA constructs to determine the impact of UCH-L1 depletion in these cells. Compared with untransduced cells and a non-silencing control, 2 of the 3 *UCHL1*-targeting shRNAs reduced UCH-L1 protein levels (Figure 6D). The 2 hairpins that reduce UCH-L1 protein selectively impair the proliferation of the GCB-DLBCL cell lines with high levels of UCH-L1 (Figure 6C-D). This indicates that, when expressed, UCH-L1 provides an oncogenic signal that promotes the proliferation of DLBCL cells. To better understand this signal, we depleted UCH-L1 and examined the impact on mTOR-AKT signaling. Compared with untransduced cells and a nonsilencing control, depletion of UCH-L1 led to increased phosphorylation of p70S6 kinase (p-$S6K^{T389}$) and reduced phosphorylation of AKT^{S473}, indicative of increased mTORC1 and reduced mTORC2 activity, respectively (Figure 6E). One of the critical targets for AKT in promoting survival is FOXO1. Phosphorylation of FOXO1 leads to its cytoplasmic sequestration and a reduction in its ability to promote the transcription of its targets. We therefore examined the level of *UCHL1* and that of a list of well-characterized FOXO1 targets in mature B-cell lymphomas. Of the 9 FOXO1 targets examined, all but 1 was

Table 2. Univariate analysis of prognostic factors

Factor	RR	95% CI	*P*
UCHL1 >80%	2.26	1.39-3.64	.0012
MYC >85%	2.21	1.18-3.87	.0148
EZH2 <85%	2.6	1.16-7.43	.0184

N = 227 cases of GCB-DLBCL uniformly treated with R-CHOP.
CI, confidence interval; RR, relative risk.

Table 3. Multivariate proportional hazard analysis of prognostic factors

Factor	RR	95% CI	P
UCHL1 >80%	2.4	1.46-3.91	.0007
MYC >85%	1.89	1.00-3.35	.0495
EZH2 <85%	3.29	1.45-9.48	.0028

N = 227 cases of GCB-DLBCL uniformly treated with R-CHOP.
Abbreviations explained in Table 2.

significantly ($P < .05$) correlated with the level of *UCHL1* (supplemental Figure 8A-B). Of these, 6 of the 9 FOXO1 targets were inversely proportional to *UCHL1*, consistent with decreased FOXO1 activity (supplemental Figure 8B-D). Taken together, these data lead us to conclude that UCH-L1 promotes AKT signaling and cell survival in DLBCL.

UCH-L1 alters gene expression and antigen-specific immunity in premalignant GCBs

To further gauge the impact of UCH-L1 on GC-derived lymphomagenesis, we performed gene expression profiling on premalignant GCBs purified from young (3-6 months) IμHABCL6 and *Uchl1*/IμHABCL6 mice (n = 3 each genotype). Transgenic UCH-L1 resulted in the differential expression ($P < .05$) of 1884 probe sets composed of 951 upregulated and 933 downregulated genes (Figure 7A-B). Of these, there were 320 or 59 probe sets changed at least 1.5- or 2-fold ($P < .05$), respectively. We next examined the correlation of the top 60 altered genes with *UCHL1* levels in mature B-cell lymphomas (n = 215). Of these, 41 of 60 showed a correlation with *UCHL1* (Figure 7C). To gain insight into the nature of these changes, we performed Ingenuity Pathway Analysis (IPA) on those significantly changed probe sets (Figure 7D). There was a strong alteration in the biological processes of cell death and survival, cell growth and proliferation, cell cycle, DNA replication, recombination, and repair, and cell morphology.

To relate these expression changes to GC biology, we compared the altered genes to a list of genes with polarized expression between the light zone and dark zone GC cells. There was a significant skewing with genes upregulated in *Uchl1*^{Tg} GCBs disproportionately being enriched in light zone cells, whereas those downregulated are enriched in dark zone cells (Figure 7E). To further explore the impact of UCH-L1 on cell death, we used the TUNEL assay to examine apoptosis. Although wild-type and IμHABCL6 mice had similar numbers of TUNEL-positive cells in splenic follicles, both *Uchl1* and *Uchl1*/IμHABCL6 double mutant mice had a significant decrease consistent with reduced cell death (Figure 7F). As apoptosis is a prominent event in the context of the GC reaction, we measured the output of the GC by measuring antigen-specific antibody responses following immunization with the T-cell–dependent antigen NP-KLH. In wild-type and *Uchl1*^{Tg} mice, we find a steady increase in anti-NP IgG1 over 14 days (Figure 7G). In contrast, we find a significant reduction in the production of anti-NP IgG1 in IμHABCL6 mice. This impaired production of IgG1 is rescued by the *Uchl1* transgene. Despite the defect in NP-specific IgG1 production, there is no significant difference in affinity maturation among the different genotypes.

Discussion

Here, we find that UCH-L1, an enzyme that was previously thought to be a specific marker of the neuroendocrine system, is induced in B cells undergoing the GC reaction and is also highly expressed in lymphomas derived from GCBs. Our prior work has revealed a novel role for UCH-L1 in regulating the prosurvival mTOR-AKT pathway both in malignant B cells and in the brain, where levels of UCH-L1 are highest. The ability of enforced UCH-L1 expression to promote spontaneous B-cell lymphoma, as well as those driven by *MYC* or *BCL6*, indicates that the prosurvival role of endogenous UCH-L1 in GCBs is rate-limiting, with higher levels able to further enhance B-cell survival and ultimately result in malignant transformation. Interestingly, our results with RNA interference suggest that in those GCB-DLBCL cells where UCH-L1 is high, it is providing an essential survival signal. The class of deubiquitinating enzymes is an emerging target for pharmaceutical compounds, with several inhibitors in preclinical development stages.[26,27] An improved understanding of the role of UCH-L1 in disease and physiology provides important insight into the potential efficacy of small-molecule inhibitors for the treatment of B-cell cancers, and helps to understand the potential physiological effects of this strategy.

GCB-DLBCL disproportionately affects children, adolescents, and young adults, with the incidence of ABC subtype increasing with patient age.[28-31] In adults, the outcome for patients with GCB disease is superior to that seen in patients with the ABC subtype.[1] In patients of all ages, relapsed disease offers a much worse prognosis, with second-line therapies able to salvage only a fraction of patients.[2,3,32-34] There are few clinical features or biomarkers that offer a robust risk-stratification option in DLBCL, particularly for those with GCB disease. Our data provide important insight into the ability to identify those with GCB disease at high risk for relapse. Future work is required to test the ability to detect high UCH-L1 on clinical samples using standard methods, and for this to predict relapse in a prospective manner.

Although this report focuses on the oncogenic role of UCH-L1 in the GC, our findings of strong induction of UCH-L1 in GCBs leads to questions about the transcriptional regulation and the potential physiological role of UCH-L1 in this compartment. Very little is known regarding the regulation of *UCHL1*, though 1 study has linked the PU.1 transcription factor (*SPI1*) with *UCHL1* transcription in B-cell lymphoma.[35] Unfortunately, the levels of *UCHL1* do not correlate with those of *SPI1* in the gene expression data sets we examined (data not shown). The level of *UCHL1* transcript and protein in B cells transitioning through the GC mirror that of the master regulator BCL6, though there is no evidence that UCH-L1 levels are directly regulated by this factor. In fact, neither BCL6 depletion, nor the overexpression of degradation-deficient BCL6, substantially changed *UCHL1* transcript levels.[21,22] ChIP-seq data further do not demonstrate BCL6 occupancy of the *UCHL1* promoter.[23] It is of course possible that BCL6 acts indirectly to stimulate *UCHL1* transcription. It will be important to further define the transcriptional regulation of UCHL1 in GCBs to better understand its role in the lymphomas arising from this structure.

Despite it being among the first deubiquitinating enzymes discovered,[20] there is a paucity of data regarding its physiological roles. We recently reported a novel function of UCH-L1 in regulating mTOR-AKT signaling.[8] High levels of enzyme drive increased assembly of mTORC2 that phosphorylates AKT^{S473}, a function that requires catalytic activity. UCH-L1 antagonizes the activity of a CUL4-DDB1 ubiquitin E3 ligase in ubiquitinating the mTORC1 subunit raptor, with reduced ubiquitination seen in the presence of UCH-L1 or after the depletion of DDB1. Several prior studies have shown that AKT is hyperphosphorylated in a substantial proportion of DLBCL and Burkitt lymphoma.[36-38] Although we have identified UCH-L1 to be one mechanism by which this may occur, there are, however, a number of other mechanisms leading to increased AKT activity in B-cell lymphoma. Recent sequencing studies have identified mutations in *CD79A/B*, *GNA13*, and *S1PR2* genes that result in increased phosphatidylinositol 3-kinase (PI3K) activity in DLBCL,[39,40] as well as loss

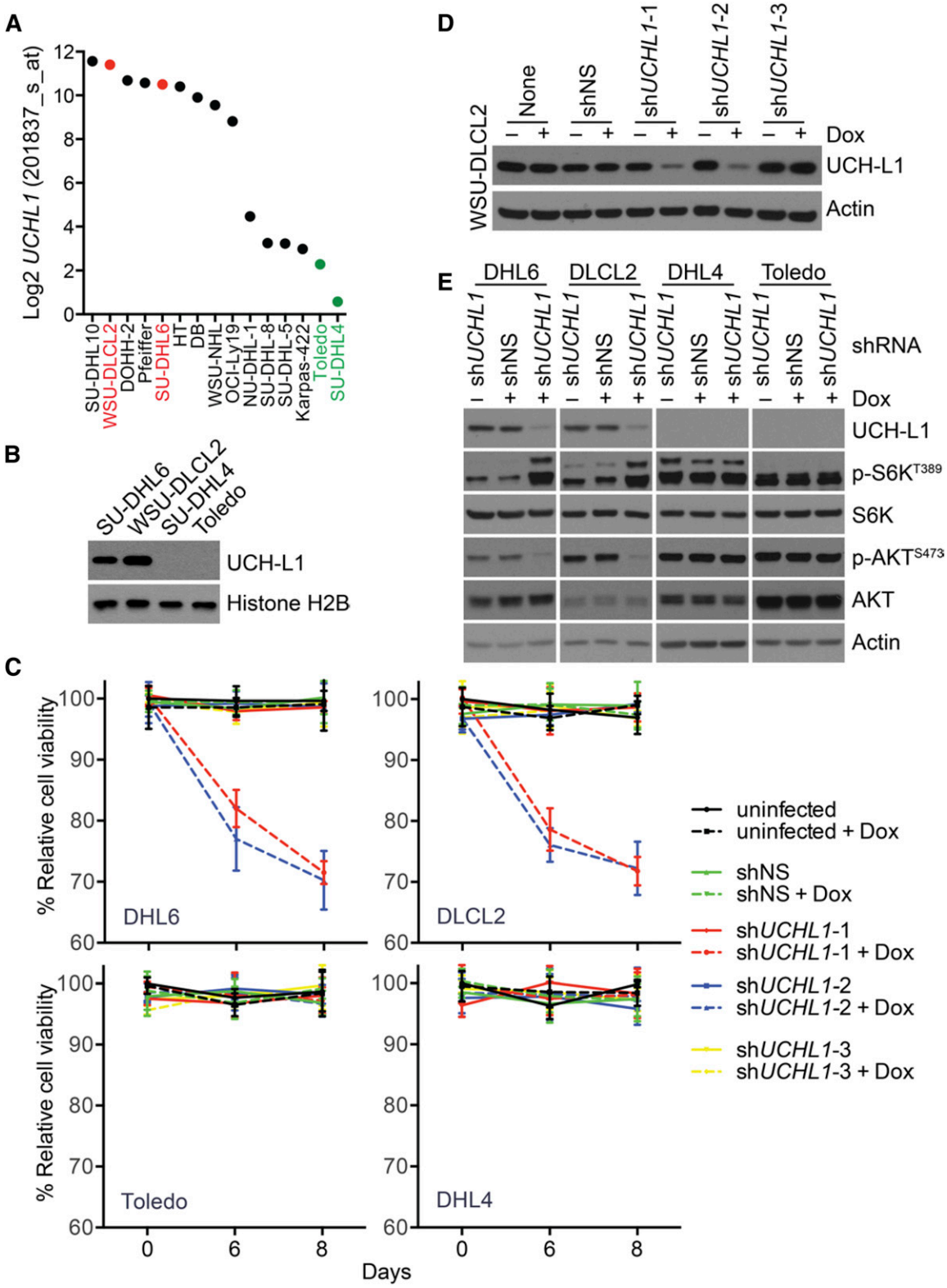

Figure 6. UCH-L1 promotes AKT phosphorylation and cell survival in DLBCL. (A) The expression of *UCHL1* is shown for a series of GCB-DLBCL cell lines. The cell lines used in this study are shown in red (*UCHL1* HI) and green (*UCHL1* LO). Data extracted from the CCLE (GSE36133) and analyzed using the R2: Genomics Analysis and Visualization Platform (http://r2.amc.nl). (B) Immunoblot analysis of the cell lines from panel A. Histone H2B is included as a loading control. (C-D) The cell lines from panel A were transduced with lentivirus' encoding the indicated Dox-inducible shRNA constructs. Cell viability (C) was monitored using the MTS assay. The level of UCH-L1 (D) is shown for the WSU-CLCL2 cell line. shNS, control nonsilencing; shUCHL1, $n = 3$ independent *UCHL1* targeting shRNA constructs. Similar results were obtained in SU-DHL6 cells. (E) The indicated cell lines were transduced with the indicated shRNA constructs as in panels C and D and the resulting extracts were analyzed with antibodies against the indicated proteins. Dox was included where indicated.

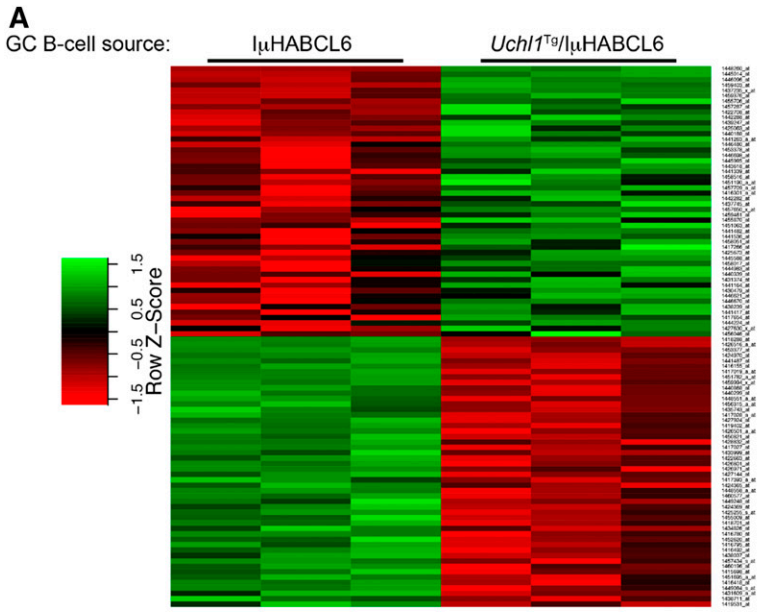

B

Up-regulated		Down-regulated	
Symbol	Fold-change	Symbol	Fold-change
Fcrl1	2.07	*Cpd*	-3.62
Dock10	1.79	*Trim2*	-2.75
Ldlr	1.64	*Sh3d19*	-2.73
Stxbp4	1.57	*Pi4k2b*	-2.61
Anxa6	1.54	*Pdia2*	-2.56
Pik3cg	1.53	*Hnrnpll*	-2.51
Lpp	1.52	*Slc39a8*	-2.44
Ccdc122	1.50	*Sept8*	-2.38
Fcer2	1.49	*Clcn2*	-2.26
Mapk6	1.48	*Trf2*	-2.23
Itprip	1.46	*Rhof*	-2.21
Prss23	1.43	*Ptpla*	-2.18
Rwdd3	1.41	*Jmy*	-2.12
Smpdl3b	1.41	*Fam132a*	-2.03
Hdac9	1.40	*Klhl23*	-1.96
Phf20	1.39	*Gabarapl1*	-1.96
Bach2	1.39	*Purg*	-1.88
Rad50	1.38	*Lpin1*	-1.86
Hoxd9	1.37	*Golm1*	-1.84
Ldhb	1.36	*Sh2d4a*	-1.82
Dpysl2	1.36	*Herc6*	-1.81
Git2	1.35	*Mb21d1*	-1.80
Tacstd2	1.35	*Gabbp2*	-1.78
Trmt13	1.34	*Pla2g4a*	-1.77
Pdp2	1.34	*Adcy9*	-1.76
Vwa5a	1.33	*Ptpla*	-1.73
Lbh	1.33	*Uba7*	-1.70
Rbm26	1.33	*Pfkm*	-1.70
Zc4h2	1.32	*Orc1*	-1.69
Scp2	1.31	*Gpx4*	-1.69

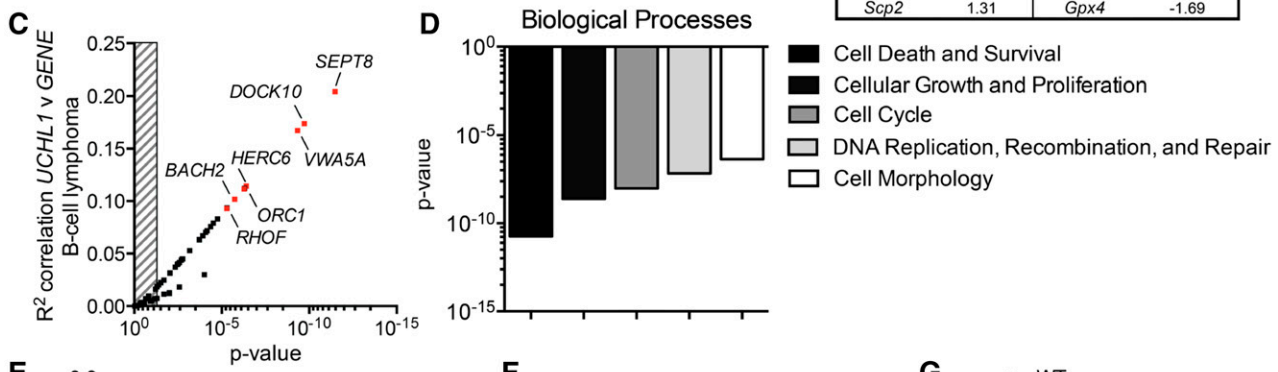

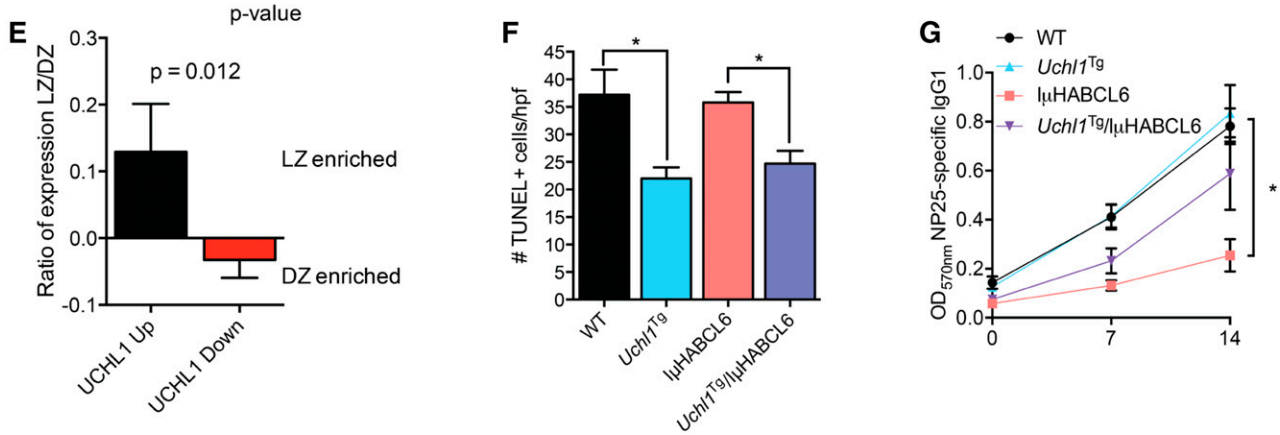

Figure 7. Transgenic UCH-L1 leads to altered gene expression in GCBs. (A-B) Gene expression profiling was performed using RNA extracted from GCBs from mice of the indicated genotypes (n = 3 each). (A) A heat map represents the relative expression of the 100 most discriminatory genes. (B) The 60 most altered genes (30 up, 30 down; $P < .01$) are shown with the mean fold-change indicated. (C) The list of genes from panel B were correlated with *UCHL1* levels in 215 mature B-cell lymphomas extracted from GSE4475[14] and analyzed using the R2: Genomics Analysis and Visualization Platform (http://r2.amc.nl). The graph represents the Pearson correlation R^2 value and the corresponding *P* value for each gene. The hatched area on the left represents a $P > .05$. Genes with the most significant correlation are indicated in red. (D) IPA was performed using the list of differentially expressed genes ($P < .05$) from panel A. The graph represents the *P* values of the top 5 altered biological processes. (E) The expression ratio (mean ± SE) of the list of top upregulated and downregulated genes from panel B in purified mouse light zone (LZ) or dark zone (DZ) cells (GSE38696[17]) is shown. The *P* value was calculated with the Student *t* test. (F) Formalin-fixed paraffin-embedded spleen sections from mice of the indicated genotypes were stained using the TUNEL assay. The graph represents the mean ± SE number of TUNEL-positive cells from 10 randomly selected high-power field (hpf) images from each of 3 mice per genotype (total of 30 hpf per genotype). *P* values were calculated with the Student *t* test. (G) Mice of the indicated genotypes (n = 6 each) were immunized with NP-CGG and the level of NP-specific IgG1 was determined by ELISA on the indicated days. *$P < .05$ (Student *t* test) for the comparison between IμHABCL6 and any of the other genotypes.

of phosphatase and tensin homolog that interferes with its ability to restrain the PI3K-dependent generation of phosphatidylinositol 3,4,5 trisphosphate.[36] Frequent mutations involving the *ID3* and *TCF3* genes also lead to increased PI3K activity in Burkitt lymphoma.[41] The varied mechanisms that lead to AKT activation make it unlikely that UCH-L1 alone acts as a marker of higher sensitivity to AKT inhibitors, but our data further underscore the importance of this pathway in B-cell transformation. Our data regarding the ability of transgenic UCH-L1 to promote the production of antigen-specific class-switched antibody in mice with deregulated BCL6 expression suggest that it may also have a role in the humoral immune response. Further work is required to better understand the nature of this effect.

Acknowledgments

The authors thank Dr Ricardo Dalla-Favera (Columbia University, New York, NY) for providing IμHABCL6 mice and Dr P. Leif Bergsagel (Mayo Clinic Cancer Center, Scottsdale, AZ) for the Vk*MYC mice. The authors thank Drs Richard Bram, Anne Novak, and Rodney Miles for critical reading of the manuscript and Dr Farhad Kosari for assistance with gene expression data.

This work was supported by the National Institutes of Health National Cancer Institute (CA151351) (P.J.G.), the Multiple Myeloma Research Foundation (P.J.G.), Gabrielle's Angel Foundation for Cancer Research (P.J.G.), the Hyundai Hope on Wheels Foundation (P.J.G.), and supported in part by the University of Iowa/Mayo Clinic Lymphoma SPORE CA97274. New gene expression data may be found through the Gene Expression Omnibus (http://www.ncbi.nlm.nih.gov/geo/) GSE76706.

P.J.G. is a former American Society of Hematology Basic Research Scholar, a past recipient of the Howard Hughes Medical Institute Physician Scientist Early Career Award, and a former Harriet H. Samuelsson Foundation Pediatric Cancer Research Scientist.

Authorship

Contribution: T.B. and S.H. performed the experiments; T.B., S.H., A.L.F., and P.J.G. interpreted experimental data; and P.J.G designed the experiments and wrote the manuscript.

Conflict-of-interest disclosure: P.J.G. receives research funding from Mission Therapeutics (Cambridge, United Kingdom) to conduct experiments that are not included in this manuscript. The remaining authors declare no competing financial interests.

Correspondence: Paul J. Galardy, Mayo Clinic, Guggenheim 15, 200 First St SW, Rochester, MN 55905; e-mail: galardy.paul@mayo.edu.

References

1. Alizadeh AA, Eisen MB, Davis RE, et al. Distinct types of diffuse large B-cell lymphoma identified by gene expression profiling. *Nature.* 2000; 403(6769):503-511.
2. Cairo MS, Gerrard M, Sposto R, et al; FAB LMB96 International Study Committee. Results of a randomized international study of high-risk central nervous system B non-Hodgkin lymphoma and B acute lymphoblastic leukemia in children and adolescents. *Blood.* 2007;109(7):2736-2743.
3. Friedberg JW. Relapsed/refractory diffuse large B-cell lymphoma. *Hematology Am Soc Hematol Educ Program.* 2011;2011:498-505.
4. Ovaa H, Kessler BM, Rolén U, Galardy PJ, Ploegh HL, Masucci MG. Activity-based ubiquitin-specific protease (USP) profiling of virus-infected and malignant human cells. *Proc Natl Acad Sci USA.* 2004;101(8):2253-2258.
5. Hussain S, Foreman O, Perkins SL, et al. The de-ubiquitinase UCH-L1 is an oncogene that drives the development of lymphoma in vivo by deregulating PHLPP1 and Akt signaling. *Leukemia.* 2010;24(9):1641-1655.
6. Srinivasan L, Sasaki Y, Calado DP, et al. PI3 kinase signals BCR-dependent mature B cell survival. *Cell.* 2009;139(3):573-586.
7. Sander S, Calado DP, Srinivasan L, et al. Synergy between PI3K signaling and MYC in Burkitt lymphomagenesis. *Cancer Cell.* 2012;22(2): 167-179.
8. Hussain S, Feldman AL, Das C, Ziesmer SC, Ansell SM, Galardy PJ. Ubiquitin hydrolase UCH-L1 destabilizes mTOR complex 1 by antagonizing DDB1-CUL4-mediated ubiquitination of raptor. *Mol Cell Biol.* 2013;33(6):1188-1197.
9. Jolly CJ, Klix N, Neuberger MS. Rapid methods for the analysis of immunoglobulin gene hypermutation: application to transgenic and gene targeted mice. *Nucleic Acids Res.* 1997;25(10): 1913-1919.
10. Cattoretti G, Pasqualucci L, Ballon G, et al. Deregulated BCL6 expression recapitulates the pathogenesis of human diffuse large B cell lymphomas in mice. *Cancer Cell.* 2005;7(5): 445-455.
11. Chesi M, Robbiani DF, Sebag M, et al. AID-dependent activation of a MYC transgene induces multiple myeloma in a conditional mouse model of post-germinal center malignancies. *Cancer Cell.* 2008;13(2):167-180.
12. Cato MH, Yau IW, Rickert RC. Magnetic-based purification of untouched mouse germinal center B cells for ex vivo manipulation and biochemical analysis. *Nat Protoc.* 2011;6(7):953-960.
13. Klein U, Tu Y, Stolovitzky GA, et al. Transcriptional analysis of the B cell germinal center reaction. *Proc Natl Acad Sci USA.* 2003; 100(5):2639-2644.
14. Hummel M, Bentink S, Berger H, et al; Molecular Mechanisms in Malignant Lymphomas Network Project of the Deutsche Krebshilfe. A biologic definition of Burkitt's lymphoma from transcriptional and genomic profiling. *N Engl J Med.* 2006;354(23):2419-2430.
15. Visco C, Li Y, Xu-Monette ZY, et al. Comprehensive gene expression profiling and immunohistochemical studies support application of immunophenotypic algorithm for molecular subtype classification in diffuse large B-cell lymphoma: a report from the International DLBCL Rituximab-CHOP Consortium Program Study. *Leukemia.* 2012;26(9):2103-2113.
16. Barretina J, Caponigro G, Stransky N, et al. The Cancer Cell Line Encyclopedia enables predictive modelling of anticancer drug sensitivity. *Nature.* 2012;483(7391):603-607.
17. Victora GD, Dominguez-Sola D, Holmes AB, Deroubaix S, Dalla-Favera R, Nussenzweig MC. Identification of human germinal center light and dark zone cells and their relationship to human B-cell lymphomas. *Blood.* 2012;120(11):2240-2248.
18. Calado DP, Sasaki Y, Godinho SA, et al. The cell-cycle regulator c-Myc is essential for the formation and maintenance of germinal centers. *Nat Immunol.* 2012;13(11):1092-1100.
19. Dominguez-Sola D, Victora GD, Ying CY, et al. The proto-oncogene MYC is required for selection in the germinal center and cyclic reentry. *Nat Immunol.* 2012;13(11):1083-1091.
20. Wilkinson KD, Lee KM, Deshpande S, Duerksen-Hughes P, Boss JM, Pohl J. The neuron-specific protein PGP 9.5 is a ubiquitin carboxyl-terminal hydrolase. *Science.* 1989;246(4930):670-673.
21. Basso K, Margolin AA, Stolovitzky G, Klein U, Dalla-Favera R, Califano A. Reverse engineering of regulatory networks in human B cells. *Nat Genet.* 2005;37(4):382-390.
22. Phan RT, Saito M, Basso K, Niu H, Dalla-Favera R. BCL6 interacts with the transcription factor Miz-1 to suppress the cyclin-dependent kinase inhibitor p21 and cell cycle arrest in germinal center B cells. *Nat Immunol.* 2005;6(10): 1054-1060.
23. Basso K, Saito M, Sumazin P, et al. Integrated biochemical and computational approach identifies BCL6 direct target genes controlling multiple pathways in normal germinal center B cells. *Blood.* 2010;115(5):975-984.
24. Aukema SM, Siebert R, Schuuring E, et al. Double-hit B-cell lymphomas. *Blood.* 2011;117(8): 2319-2331.
25. Lee HJ, Shin DH, Kim KB, et al. Polycomb protein EZH2 expression in diffuse large B-cell lymphoma is associated with better prognosis in patients treated with rituximab, cyclophosphamide, doxorubicin, vincristine and prednisone. *Leuk Lymphoma.* 2014;55(9):2056-2063.
26. Peterson LF, Sun H, Liu Y, et al. Targeting deubiquitinase activity with a novel small-molecule inhibitor as therapy for B-cell malignancies. *Blood.* 2015;125(23):3588-3597.
27. Kapuria V, Peterson LF, Fang D, Bornmann WG, Talpaz M, Donato NJ. Deubiquitinase inhibition by small-molecule WP1130 triggers aggresome formation and tumor cell apoptosis. *Cancer Res.* 2010;70(22):9265-9276.
28. Deffenbacher KE, Iqbal J, Sanger W, et al. Molecular distinctions between pediatric and adult

mature B-cell non-Hodgkin lymphomas identified through genomic profiling. *Blood.* 2012;119(16): 3757-3766.

29. Klapper W, Kreuz M, Kohler CW, et al; Molecular Mechanisms in Malignant Lymphomas Network Project of the Deutsche Krebshilfe. Patient age at diagnosis is associated with the molecular characteristics of diffuse large B-cell lymphoma. *Blood.* 2012;119(8):1882-1887.
30. Miles RR, Raphael M, McCarthy K, et al; SFOP/LMB96/CCG5961/UKCCSG/NHL 9600 Study Group. Pediatric diffuse large B-cell lymphoma demonstrates a high proliferation index, frequent c-Myc protein expression, and a high incidence of germinal center subtype: Report of the French-American-British (FAB) international study group. *Pediatr Blood Cancer.* 2008;51(3):369-374.
31. Oschlies I, Klapper W, Zimmermann M, et al. Diffuse large B-cell lymphoma in pediatric patients belongs predominantly to the germinal-center type B-cell lymphomas: a clinicopathologic analysis of cases included in the German BFM (Berlin-Frankfurt-Munster) Multicenter Trial. *Blood.* 2006;107(10):4047-4052.
32. Feugier P, Van Hoof A, Sebban C, et al. Long-term results of the R-CHOP study in the treatment of elderly patients with diffuse large B-cell lymphoma: a study by the Groupe d'Etude des Lymphomes de l'Adulte. *J Clin Oncol.* 2005; 23(18):4117-4126.
33. Rovira J, Valera A, Colomo L, et al. Prognosis of patients with diffuse large B cell lymphoma not reaching complete response or relapsing after frontline chemotherapy or immunochemotherapy. *Ann Hematol.* 2015;94(5):803-812.
34. Griffin TC, Weitzman S, Weinstein H, et al; Children's Oncology Group. A study of rituximab and ifosfamide, carboplatin, and etoposide chemotherapy in children with recurrent/refractory B-cell (CD20+) non-Hodgkin lymphoma and mature B-cell acute lymphoblastic leukemia: a report from the Children's Oncology Group. *Pediatr Blood Cancer.* 2009;52(2):177-181.
35. Bheda A, Yue W, Gullapalli A, Shackelford J, Pagano JS. PU.1-dependent regulation of UCH L1 expression in B-lymphoma cells. *Leuk Lymphoma.* 2011;52(7):1336-1347.
36. Pfeifer M, Grau M, Lenze D, et al. PTEN loss defines a PI3K/AKT pathway-dependent germinal center subtype of diffuse large B-cell lymphoma. *Proc Natl Acad Sci USA.* 2013;110(30): 12420-12425.
37. Hasselblom S, Hansson U, Olsson M, et al. High immunohistochemical expression of p-AKT predicts inferior survival in patients with diffuse large B-cell lymphoma treated with immunochemotherapy. *Br J Haematol.* 2010; 149(4):560-568.
38. Uddin S, Hussain AR, Siraj AK, et al. Role of phosphatidylinositol 3′-kinase/AKT pathway in diffuse large B-cell lymphoma survival. *Blood.* 2006;108(13):4178-4186.
39. Muppidi JR, Schmitz R, Green JA, et al. Loss of signalling via Gα13 in germinal centre B-cell-derived lymphoma. *Nature.* 2014;516(7530): 254-258.
40. Davis RE, Ngo VN, Lenz G, et al. Chronic active B-cell-receptor signalling in diffuse large B-cell lymphoma. *Nature.* 2010;463(7277): 88-92.
41. Schmitz R, Young RM, Ceribelli M, et al. Burkitt lymphoma pathogenesis and therapeutic targets from structural and functional genomics. *Nature.* 2012;490(7418):116-120.